ACS SENSORS

Article

Cite This: ACS Sens. XXXX, XXX, XXX−XXX

pubs.acs.org/acssensors

Protein−Polymer Block Copolymer Thin Films for Highly Sensitive Detection of Small Proteins in Biological Fluids

Justin M. Paloni, Xue-Hui Dong, and Bradley D. Olsen*

Department of Chemical Engineering, Massachusetts Institute of Technology, Cambridge, Massachusetts 02139, United States

Supporting Information

ABSTRACT: In nearly all biosensors, sensitivity is greatly reduced for measurements conducted in biological matrices due to nonspecific binding from off-target molecules. One method to overcome this issue is to design a sensor that enables selective size-based uptake of proteins. Herein, a protein−polymer conjugate thin-film biosensor is fabricated that self-assembles into lamellae containing alternating domains of protein and polymer. Analyte is captured in protein regions while polymer domains restrict diffusion of large molecules. Device sensitivity and size-based exclusion properties are probed using two analytes: streptavidin (SA, 52.8 kDa) and monomeric streptavidin (mSA2, 15.6 kDa). Tuning domain spacing by adjusting polymer molecular weight allows the design of films that relatively freely uptake mSA2 and largely restrict SA diffusion. Furthermore, when detecting the smaller mSA2, no reduction in the limit of detection (LOD) is observed when transitioning from detection in the buffer to detection in biological fluids. As a result, LOD measured in fluid samples is reduced by 2 orders of magnitude compared to a traditional surface-immobilized protein monolayer.

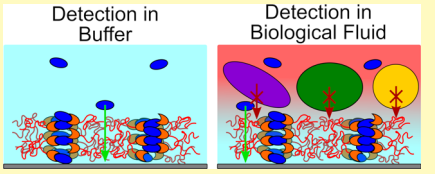

KEYWORDS: *biosensor, size-based diffusion, block copolymer, bioconjugate, sandwich ELISA*

Proteins such as antibodies[1] and other high-affinity binders[2,3] have seen widespread use as molecular recognition elements in biosensors due to their ability to bind a specific analyte with high sensitivity and selectivity. After the analyte is captured in a biosensor, this binding event is converted into a detectable signal using one of a variety of mechanisms including colorimetric signal,[4] electrical signal,[5] or optical measurements.[6−8] For each of these detection techniques, however, nonspecific binding from off-target molecules increases the background signal, which can increase the limit of detection (LOD) by orders of magnitude.[9,10] This noise issue is particularly problematic in blood, urine, and other biological matrices commonly used for analysis, which can contain molecules present at concentrations billions of times greater than the target analyte.[9] While methods have been developed to at least partially overcome nonspecific binding problems, such as by developing biosensor surface morphologies that significantly enhance specificity for an analyte,[11,12] coating the biosensor surface with a hydrogel layer or Nafion membrane,[13] or using magnetic beads for detection,[14,15] these methods either have long-term stability issues or increase biosensor complexity, thereby decreasing robustness.

One potentially simple method to reduce nonspecific binding in biosensors is through size-based exclusion. Though preventing molecules significantly larger than the target analyte from contacting the binding sites in a biosensor has been demonstrated to improve device sensitivity, current technologies have primarily focused on separating small molecules from proteins[16,17] or proteins from red blood cells.[18,19] Comparatively few methods have been investigated to selectively detect small proteins in biological matrices despite the presence of many relevant protein biomarkers that are smaller than 15 kDa including markers for sepsis,[20] heart failure,[21] and Alzheimer's disease.[22] These molecules are all significantly smaller than the majority of proteins in blood[23] and urine,[24] providing a potential route for selective matrix detection of these small proteins via size-exclusion methods.

Entropic repulsion of large proteins has been demonstrated using a variety of polymeric materials. One of the most commonly used techniques to prevent nonspecific adsorption of large proteins onto a biosensor surface is through grafting polymer brushes onto the device.[25−27] Similar protein exclusion properties have been observed in vesicles coated with a polymer brush exterior.[28,29] As polymer brush density increases, the maximum size of a protein that can diffuse into the brush decreases,[30] which is consistent with theoretical predictions.[31] Size-exclusion behavior has also been observed in hydrogels, in which smaller mesh sizes have been found to increase the frictional force experienced by molecules diffusing through the gel[32,33] and cause exclusion of particles sufficiently larger than this mesh size.[34] Although the various aforementioned methods of entropic protein repulsion are effective at excluding these molecules, the techniques have not been incorporated into a biosensor for the purpose of differentiating between differently sized proteins.

One material that could simultaneously provide size-based exclusion of proteins and act as an effective biosensor is a protein−polymer conjugate thin film. The self-assembly of protein−polymer conjugates has been extensively studied,[35−40]

Received: June 3, 2019
Accepted: September 26, 2019

DOI: 10.1021/acssensors.9b01020
ACS Sens. XXXX, XXX, XXX−XXX

Scheme 1. Bioconjugation of 3xSso Containing an N-Terminal Cysteine Residue to Maleimide-Functionalized PNIPAM[a]

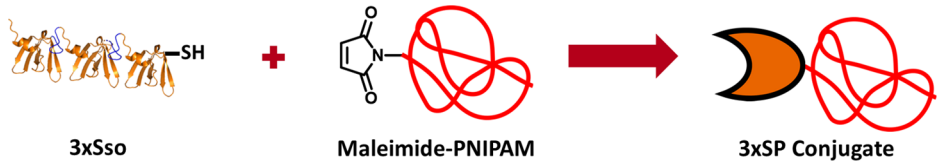

[a]Orange regions in 3xSso are cartoon representations of the Sso7d crystal structure generated using Protein Data Bank ID 1SSO.[47]

revealing that these materials assemble analogously to traditional diblock copolymers with an enhanced range of conditions over which lamellae are formed.[36] Within these lamellar nanostructures, domains of densely packed protein and polymer serve as regions that can allow analyte binding and control diffusion into the material using size-based exclusion, respectively. When cast into thin films, protein−polymer conjugates contain binding sites throughout the entire three-dimensional structure of the film, allowing enhanced sensitivity compared to traditional biosensors utilizing surface-immobilized proteins due to the larger effective areal density of binding sites.[35,41] Additionally, antibody−polymer conjugate thin films were observed to permit diffusion of protein G (22 kDa) into the film, but excluded a horseradish peroxidase-protein G fusion protein (66 kDa),[41] providing evidence for a size-based exclusion mechanism for diffusion.

In this work, the size-exclusion properties of protein−polymer conjugate thin films are studied by varying the molecular weight of the polymer block and the analyte. Shorter polymer blocks and larger analyte size are found to restrict diffusion into the films more. Furthermore, no decrease in the limit of detection is observed when using a small analyte (15.6 kDa) or when transitioning from detection in the buffer to that in biological fluids (blood and urine). The excellent sensitivity in these fluids is attributed to the exclusion of larger molecules in the fluids as well as the relatively enhanced diffusion rate of the small analyte into the film. A model sandwich assay is also designed for the protein−polymer conjugate thin film, indicating the feasibility of performing an enzyme-linked immunosorbent assay (ELISA) using this biosensor architecture.

MATERIALS AND METHODS

Materials. All solvents were purchased from VWR, and all other chemicals were purchased from MilliporeSigma and used without further purification. Streptavidin labeled with Alex Fluor 647, biotinylated horseradish peroxidase (biotin-HRP), and Alex Fluor 647 and 488 NHS esters were purchased from Thermo Fisher Scientific. Whole blood was purchased from Research Blood Components, LLC. Bovine serum albumin (BSA) was purchased from MilliporeSigma. Unlabeled streptavidin was purchased from New England Biolabs. Silicon wafers were purchased from Wafer World, and quartz slides were purchased from Ted Pella, Inc.

Polymer Synthesis, Protein Expression, and Bioconjugation. Details of polymer synthesis, protein expression, and bioconjugation reactions between polymer and protein are described in the Supporting Information.

Thin Film Preparation. Silicon wafers (P-type silicon with boron as a dopant, (100) orientation, single-side polished) cut into rectangular sections or quartz slides (only used in experiments for which binding intensity was measured as a function of film thickness) were sequentially rinsed with acetone, methanol, and water. Substrates were then dried under a filtered airflow and treated with oxygen plasma for 3 min. Immediately following plasma cleaning, conjugate samples rehydrated to 10 wt % in Milli-Q water were flow coated onto the substrates in a chamber maintained at 60% relative humidity, as described previously.[42] To stabilize thin films against dissolution in water, the cast films were preheated to 40 °C and immersed in a 1.4 wt % aqueous solution of glutaraldehyde at 40 °C for 20 s to lightly cross-link the protein nanodomains. Immediately following immersion, thin films were thoroughly rinsed with water until the surfaces became hydrophilic, indicating complete removal of unlinked glutaraldehyde. Films were dried under filtered air and stored at ambient conditions until use. Film thickness was determined using a Woolam M-2000D spectroscopic ellipsometer using a single-incidence angle of 70°. Curves were fit using a three-layer model consisting of a 0.4 mm bottom silicon substrate, a native silicon oxide layer of 1.8 nm, and a top conjugate layer fit using a Cauchy model. Thin films were characterized using grazing-incidence small-angle X-ray scattering (GISAXS) as described in the Supporting Information. rcSso7d.SA (Sso) monolayers were prepared by coupling protein activated by 1-ethyl-3-(3-dimethylaminopropyl)carbodiimide/*N*-hydroxysuccinimide (EDC/NHS) with amine-functionalized silicon wafers using literature methods.[43]

Fluorescent Assays. The binding capabilities of Sso monolayers and conjugate thin films were measured using fluorescently labeled streptavidin (SA) and monomeric streptavidin (mSA2). Details of the expression, purification, and fluorescent labeling of mSA2 are provided in Supporting Information. Samples were prepared by serial dilution of SA or mSA2 in PBS (pH 7.4), human urine (diluted to 50% v/v in PBS, pH 7.4), or blood serum (obtained as the supernatant by centrifuging whole blood at 1500*g* for 10 min, and then diluted to 50% v/v in PBS, pH 7.4). These solutions were gently applied to the surface of a bioconjugate thin film or an Sso monolayer as 0.5 μL drops. Films were incubated for a specified period of time in a sealed chamber saturated with water vapor at room temperature to prevent drying of the applied fluorescent samples. The films were then rinsed with water for 10 seconds (a time determined to be sufficient to remove unbound molecules from the film) (Figure S4), dried under filtered air, and immediately analyzed for a fluorescent signal. Fluorescence microscopy images were acquired at 4× magnification using a Cy5 filter set and exposure time of 5000 ms on an Olympus IX-81 inverted fluorescence microscope with an AxioCam HRC CCD camera. Fluorescent intensity was calculated using ImageJ software[44] by determining the average fluorescent signal in a rectangular area of the fluorescent image free of defects and occupying no less than half of the full sample application area. The corrected intensity was determined by subtracting the fluorescent intensity of a sample from that of an area on the substrate far away from regions exposed to fluorescent samples.

Sandwich Assays. Bioconjugate thin films and Sso monolayers were cut into 0.25 cm × 0.25 cm pieces and securely fastened to the bottom of Falcon polystyrene 12-well plates using double-sided carbon tape. Each well was submerged in 1 mL of 1% BSA in Milli-Q water, and the 12-well plate was incubated at 37 °C for 30 min. The wells were rinsed twice by adding 2 mL of Milli-Q water and by gently shaking the well plate at 70 rpm for 5 min. Streptavidin (1 mL) diluted in PBS, urine, or blood serum (prepared as described in the Fluorescent Assays section) containing 0.1% BSA was then added to each well, and the well plate was shaken at 70 rpm for 4 h at room temperature. Wells were rinsed twice with 2 mL of Milli-Q water and then twice with 2 mL of 0.1% BSA in Milli-Q water by shaking at 70 rpm for 5 min. After rinsing, wells were submerged in 1 mL of 200 ng/mL biotin-HRP in Milli-Q water containing 0.1% BSA, and the

DOI: 10.1021/acssensors.9b01020
ACS Sens. XXXX, XXX, XXX−XXX

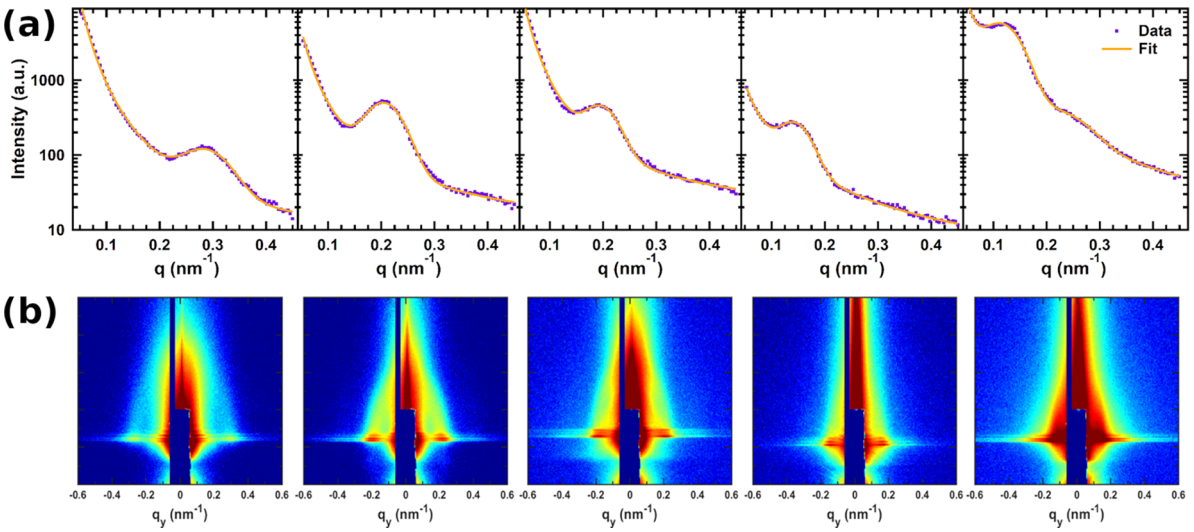

Figure 1. (a) Fit GISAXS horizontal linecuts used to calculate domain spacing in swollen thin films and (b) corresponding GISAXS patterns. In both (a) and (b), images represent data for 3xSP9.6k, 3xSP23.3k, 3xSP30.3k, 3xSP56.1k, and 3xSP77.6k from left to right. GISAXS patterns were collected at an incident angle of 0.140°.

well plate was shaken at 70 rpm for 1 h at room temperature. Wells were then rinsed with water and 0.1% BSA as described previously. One milliliter of the solution from a Pierce TMB substrate kit (Thermo Fisher Scientific) was added to each well, and the well plate was shaken vigorously at 125 rpm for 15 min at room temperature. One milliliter of 2 M H_2SO_4 was added to each well, and the absorbance at 450 nm was read using a Tecan Infinite M200 PRO plate reader.

RESULTS AND DISCUSSION

Characterizing Diffusion into Biosensor Thin Films. Protein−polymer conjugate thin films were fabricated with a wide range of domain spacings to control diffusion into the films. Each conjugate was synthesized from a previously reported trimer of rcSso7d.SA (3xSso),[35] a modified DNA-binding protein with high binding affinities for streptavidin (SA)[45] and a monomeric variant of streptavidin (mSA2),[35,46] conjugated to poly(*N*-isopropylacrylamide) (PNIPAM; Scheme 1). Thin films created using these conjugates all adopted a weak lamellar morphology (Figure 1) with domain spacings ranging from approximately 20 to 55 nm (Table 1)

Table 1. Composition of 3xSso−PNIPAM Conjugates

conjugate	PNIPAM M_n (kDa)	PNIPAM $Đ$	protein weight fraction	domain spacing[a] (nm)
3xSP9.6k	9.6	1.05	0.72	21.9
3xSP23.3k	23.3	1.06	0.52	30.6
3xSP30.3k	30.3	1.08	0.45	32.0
3xSP56.1k	56.1	1.11	0.31	43.5
3xSP77.6k	77.6	1.13	0.24	53.9

[a]Calculated from GISAXS horizontal linecuts (Figure 1a).

when swollen with water. Lamellar spacing was only observed in horizontal linecuts to GISAXS data (Figure 1), not in vertical linecuts (Figure S5), suggesting that the lamellae adopted a predominantly perpendicular orientation. The film domain spacings were consistently larger than those measured in dry bulk conjugate samples (Figure S6, Table S1), presumably due to the swelling of PNIPAM causing an expansion of domains in the films.

Fluorescent assays performed on the thin films revealed gradual uptake of the analyte. To assess the effects of analyte size on diffusion into the films, the two aforementioned analytes that could be detected by the biosensor, SA (52.8 kDa) and mSA2 (15.6 kDa), were fluorescently labeled and exposed to the films for a prescribed time. The thin films were then rinsed, and measured for fluorescent intensity indicative of protein bound to the film. These experiments were also run using a monolayer of rcSso7d.SA (Sso) immobilized onto a surface, allowing a direct comparison between the thin films and traditional surfaced-immobilized protein biosensors. Both SA and mSA2 displayed a continuous uptake into the ∼160 nm films over at least 8 h, whereas the monolayers were observed to equilibrate with the protein solution after 30 min (Figure 2). Film structure and domain spacing were not found to change as a result of film swelling over an 8 h time period (Figure S7), suggesting that films remained stable throughout the experiment. It is worth noting that the film exposed to SA reached the same intensity observed in a monolayer after ∼4.5 h, while the thin film exposed to mSA2 reached this intensity after only ∼2.5 h. These results are consistent with the idea that analyte size controls diffusion into these conjugate thin films. For a given domain spacing, a smaller molecule, such as mSA2, should experience less restricted diffusion into the films than a larger molecule, such as SA, due to the easier uptake of the smaller molecule into the polymer nanodomains (Figure 3a). Similarly, all molecules would be expected to diffuse into the films more quickly as domain spacing increases (Figure 3b). Because SA displayed slower uptake than mSA2 (relative to a monolayer) into films with the same domain spacing, it appears that the analyte size does indeed affect the uptake rate. Thus, even this initial experiment provided evidence that the larger SA molecule experienced greater resistance to diffusion into the bioconjugate films than mSA2.

Larger domain spacings allowed faster diffusion into the thin films. Fluorescent assays were again run with both SA and mSA2, but films were exposed to protein solution for only 30 min to study diffusion into the thin films at early time points prior to saturation at equilibrium binding conditions. The fluorescent intensity remained constant with increasing film

DOI: 10.1021/acssensors.9b01020
ACS Sens. XXXX, XXX, XXX−XXX

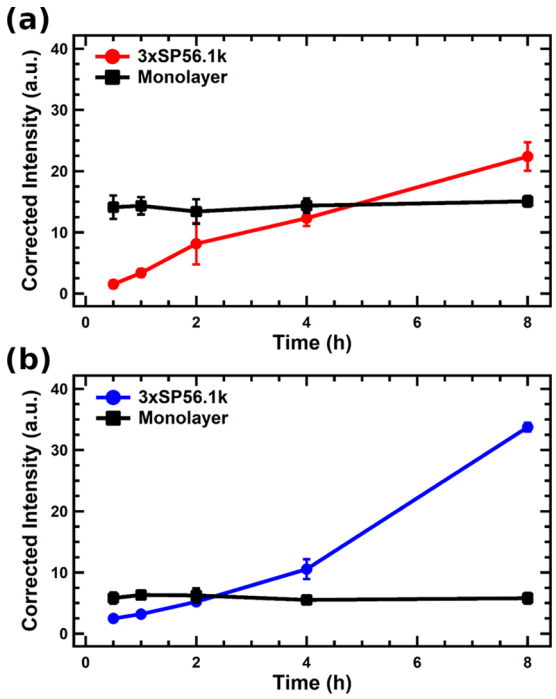

Figure 2. Fluorescent assays indicating the diffusion of (a) SA and (b) mSA2 into bioconjugate thin films over time. The film in (a) was 152 nm thick and exposed to an 800 nM solution of SA, and the film in (b) was 166 nm thick and exposed to an 800 nM solution of mSA2. Results are compared to those obtained using an Sso monolayer. Error bars represent the standard deviation of three replicates.

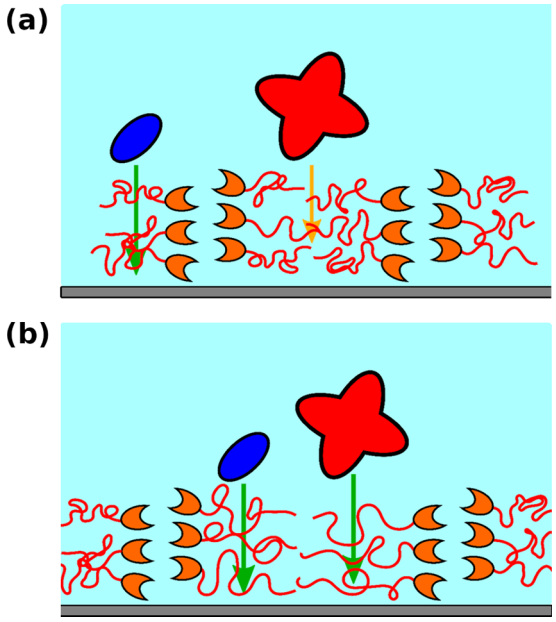

Figure 3. Diagram of SA (red) and mSA2 (blue) diffusion into 3xSP conjugate thin films with (a) a small domain spacing and (b) a larger domain spacing. Green arrows represent relatively quick diffusion into the film, while yellow arrows represent greatly restricted diffusion.

thickness for films with the smallest domain spacings when using SA as the analyte (Figure 4a). This behavior suggests that SA is only able to diffuse a small distance (less than the thickness of the shortest thin film) into the films within 30 min, resulting in SA only binding in a region at the surface of each film. Only in thin films constructed from 3xSP77.6k, which had the largest domain spacing, was an increase in signal with film thickness observed when using SA as the analyte (Figure 4b). In these films, SA is seemingly capable of diffusing through the entire thin film, causing this analyte to come into contact with and bind to more binding sites in thicker films. Because this less restricted diffusion was only observed in the films with the largest domain spacing, these findings further support the idea that domain spacing controls diffusion into the films.

Film thickness measurements conducted using mSA2 as the analyte indicated that this smaller protein experienced less restricted diffusion into thin films. In contrast to the constant intensity observed when using SA, films with the four smallest domain spacings all showed an increase in fluorescent intensity with film thickness (Figure 4c). As such, the analyte could fully access the binding sites within thin films with a significantly smaller domain spacing when mSA2 was used as the analyte (21.9 nm) than when SA was used (53.9 nm). Furthermore, when using mSA2, no change in the signal with film thickness was found for 3xSP77.6k thin films (Figure 4d). It is possible that, due to the significantly lower density of binding sites within the 3xSP77.6k films resulting from the low mass fraction of protein in this conjugate (Table 1), the greater intensity from increased mSA2 binding is difficult to detect. Indeed, only a very small increase in signal was observed with increasing film thickness when SA was added to these same thin films (Figure 4b). On the whole, however, the different binding patterns when using mSA2 and SA strongly suggest that the smaller size of mSA2 permitted easier diffusion into the films.

Biosensing Capabilities. *Sensing in Buffer.* To evaluate how the apparent size-based diffusion properties translated to biosensing capabilities, binding curves were measured using SA and mSA2 solutions in the buffer. Binding curves were fit with a quadratic model described in the Supporting Information that is a function of three parameters: the average MFI per binding event α, the total concentration of binding sites $[P]_T$, and the apparent dissociation constant $K_{d,app}$ describing the binding equilibrium between analyte and binding sites within the thin film. Best-fit values for these parameters are provided in Table S2. Nearly all independent fits gave 95% confidence intervals for α that contained the value 100 MFI/nM, demonstrating good self-consistency of the model. Limit of detection (LOD) was calculated as the concentration along the binding curve at which the measured intensity was three times the standard deviation of a blank sample measured on the same film.

An Sso monolayer, in general, outperformed the 3xSso-PNIPAM biosensor thin films when exposed to SA solutions (Figure 5a). The sensitivity of films fabricated from conjugates with the smallest domain spacing (3xSP9.6k) was over an order of magnitude lower after 30 min of exposure and approximately 2-fold higher after 4 h of exposure compared to a monolayer (Figure 5b). These results are consistent with findings that 3xSP9.6k films significantly restricted SA diffusion (Figure 4a). In contrast, 3xSP77.6k films that allowed much less restricted transport of SA (Figure 4b) were found to approach the sensitivity of a monolayer after 4 h and displayed slightly enhanced sensitivity after 8 h, demonstrating the positive effect of enhanced SA diffusivity on device performance. This improved diffusivity in 3xSP77.6k films is best demonstrated by comparing the 30 min data for the two conjugate films. Because the 3xSP77.6k film has a significantly

DOI: 10.1021/acssensors.9b01020
ACS Sens. XXXX, XXX, XXX−XXX

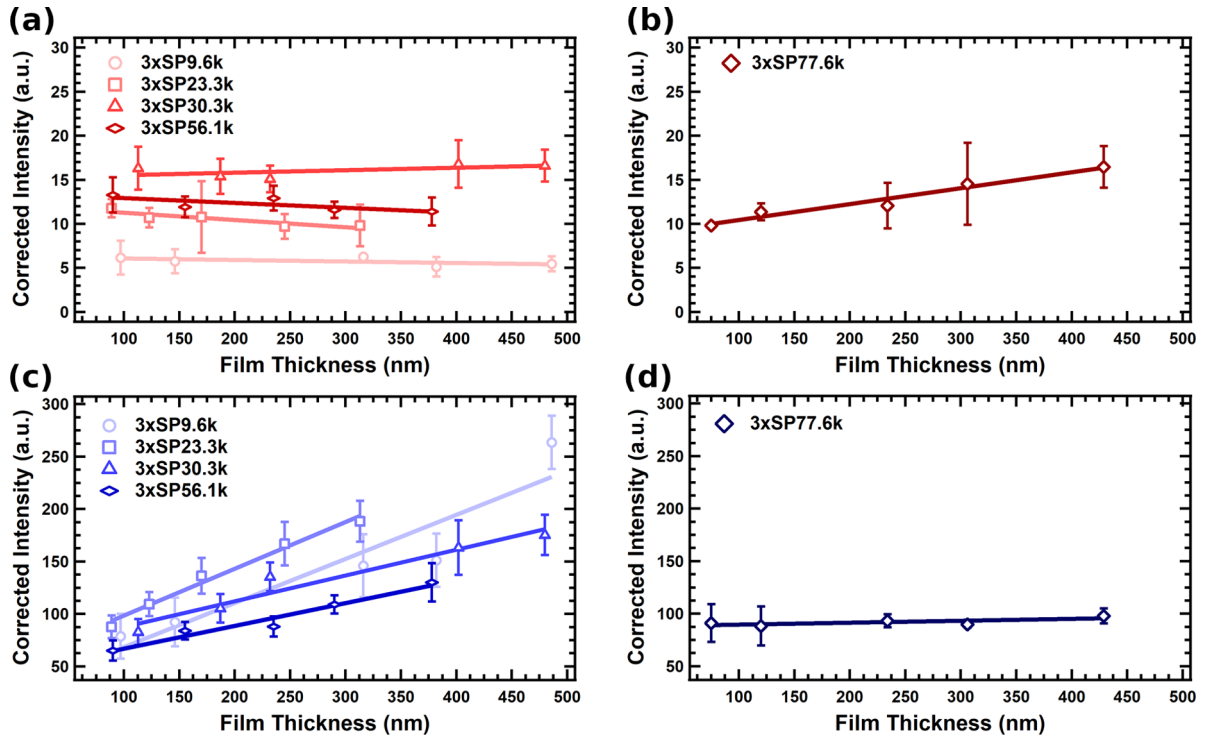

Figure 4. Results of 30-min fluorescent binding assays performed in bioconjugate thin films using (a, b) SA or (c, d) mSA2 as the analyte. Films were cast on quartz slides to reduce background signal. Graphs are divided to differentiate between films with (a, c) low M_n PNIPAM and similar behavior and (b, d) high M_n PNIPAM and similar behavior. Lines in the figure are drawn to guide the eye. The films were exposed to a 4 μM solution of (a, b) SA or (c, d) mSA2. Error bars represent the standard deviation of three replicates.

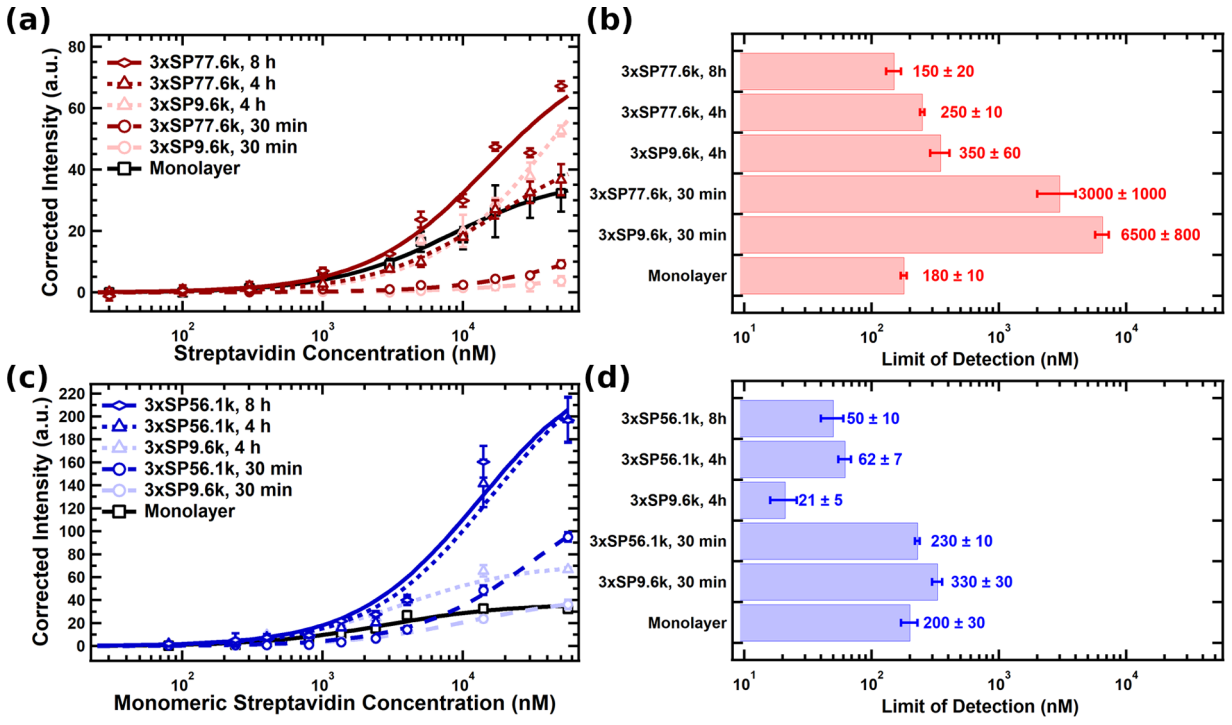

Figure 5. Binding curves for conjugate thin films exposed to (a) SA or (c) mSA2 in PBS for different periods of time. Results are compared to those obtained using an Sso monolayer with 4-h exposure time. The limit of detection determined for each binding curve is reported for films exposed to (b) SA or (d) mSA2. Film thicknesses are listed in Table S2. Error bars represent the standard deviation of three replicates.

lower density of binding sites than the 3xSP9.6k film, it would be expected that at equilibrium, the 3xSP9.6k film would display a significantly stronger fluorescent signal. Since, instead, the 3xSP77.6k thin film shows a greater fluorescent intensity after 30 min (prior to reaching equilibrium), it is likely that SA has a greater diffusivity in this film, enabling the protein to penetrate further into the film within this short time frame. In fact, the binding curve fits reveal that nearly four

DOI: 10.1021/acssensors.9b01020
ACS Sens. XXXX, XXX, XXX−XXX

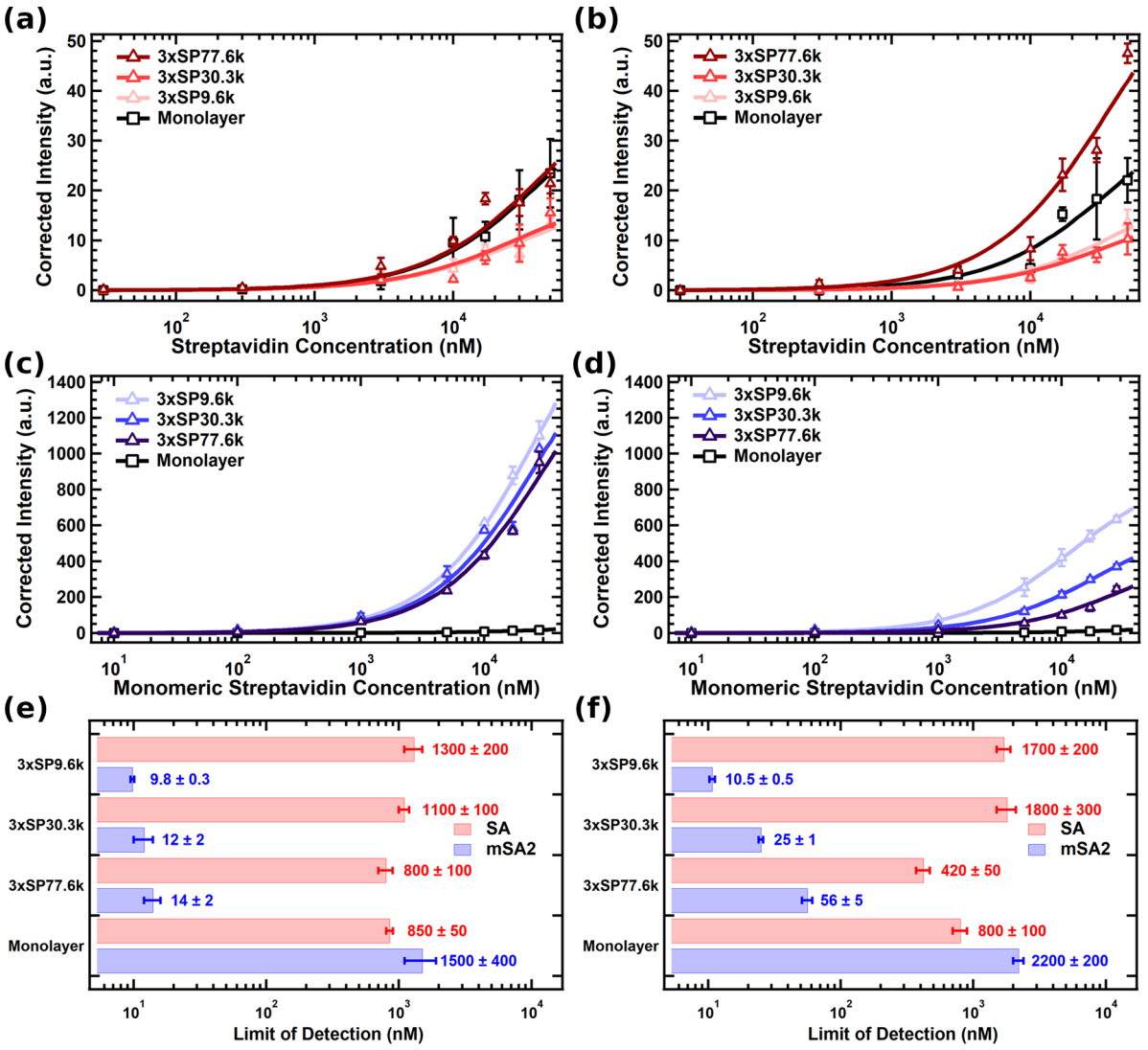

Figure 6. Binding curves for conjugate thin films exposed to (a, b) SA or (c, d) mSA2 in (a, c) 50% urine or (b, d) 50% blood serum solutions for 4 h. Results are compared to those obtained using an Sso monolayer with 4-hour exposure time. The limit of detection determined for each binding curve is reported for (e) urine samples and (f) blood samples. Film thicknesses are listed in Table S3. Error bars represent the standard deviation of three replicates.

times as many binding sites are accessed in the 3xSP77.6k film after 30 min, despite the lower total concentration of binding sites in this film (Table S2). Both films, though, demonstrate an increased number of accessible binding sites and $K_{d,app}$ value (which approaches but does not reach the monolayer value) over time. These observations are reasonable, as SA would be expected to further diffuse into the film over time, gradually accessing more binding sites and approaching the equilibrium value for the bound analyte concentration. This slow approach to equilibrium binding conditions is also consistent with the finding that thin films require significantly more time to saturate than a simple protein monolayer (Figure 2a). Overall, these results indicate that compared to a monolayer, SA is largely excluded from the thin films due to reduced diffusivity, and the diffusion properties can be tuned by changing domain spacing.

When using mSA2 as the analyte, the studied protein–polymer conjugate thin films displayed enhanced sensitivity compared to a protein monolayer. 3xSP9.6k films and 3xSP56.1k films were used to compare the biosensing capabilities of films that allowed complete mSA2 diffusion (Figure 4c) but have a large difference in the density of binding sites. While both films achieved a lower LOD than the Sso monolayer after 4 h (Figure 5c,d), using the film with a smaller domain spacing (3xSP9.6k, a 10-fold reduction in LOD) reduced the LOD more than using the film with the larger domain spacing (3xSP56.1k, a ~4-fold reduction in LOD). As the opposite trend was found when using SA, mSA2 is likely small enough relative to the domain spacing in 3xSP9.6k films such that the reduction in diffusivity compared to that in 3xSP56.1k films is not large enough to overcome the sensitivity-enhancing effect of the greater density of binding sites. This effect, however, is not a result of mSA2 accessing more binding sites in the 3xSP9.6k film, as over four times the number of binding sites are accessible in the 3xSP56.1k films (Table S2). Instead, it appears that the enhanced sensitivity results from a lower $K_{d,app}$ value within the 3xSP9.6k film (Table S2), indicating that a greater fraction of mSA2 remains bound to these films. Thus, unlike when detecting SA, the thin-

DOI: 10.1021/acssensors.9b01020
ACS Sens. XXXX, XXX, XXX−XXX

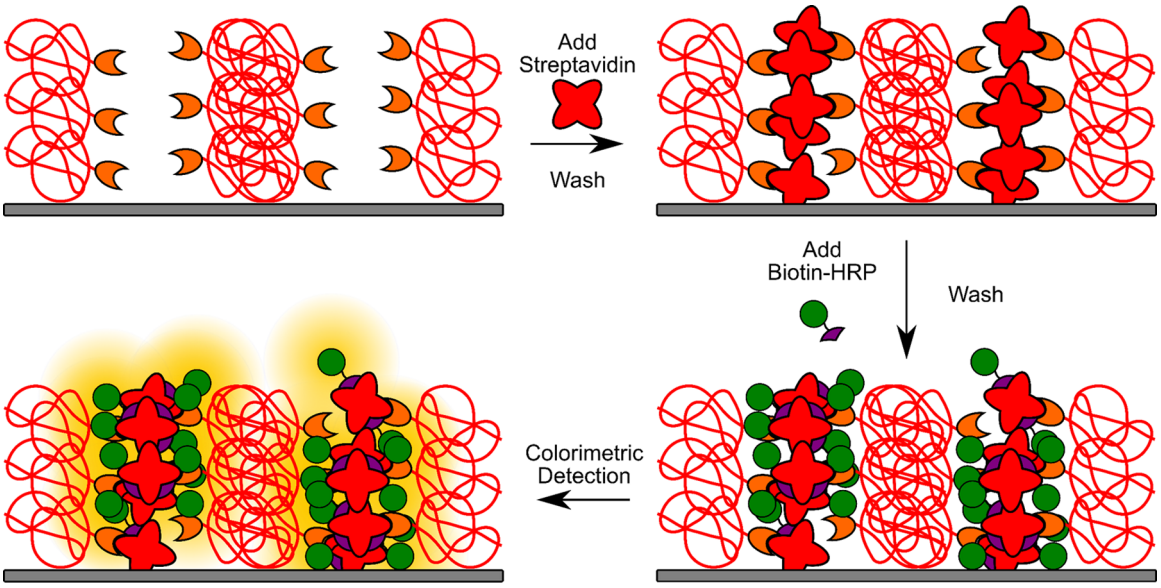

Figure 7. Schematic of model sandwich assay performed in conjugate thin-film biosensors.

film biosensors were able to effectively uptake and bind the smaller protein mSA2.

Sensing in Biological Fluids. Binding curve measurements in blood serum and urine (both 50% diluted) demonstrated that the size-based exclusion properties of the conjugate thin films could enable enhanced selectivity in biological fluids. 3xSP9.6k, 3xSP30.3k, and 3xSP77.6k films were used for these experiments, allowing comparison of device sensitivity using a range of domain spacings. When detecting SA, the thin films in general performed comparably to a monolayer (Figure 6a,b). In both blood serum and urine, the monolayers and most thin-film samples experienced an approximate 4- to 5-fold increase in LOD compared to measurements in the buffer as a result of nonspecific binding from other molecules in the fluid (Figures 5b, 6e,f). Correspondingly, the binding events in each film could be described by a $K_{d,app}$ value ∼4−5 times that of the monolayer value in the buffer (Table S3). In fact, nearly all films were found to have the same concentration of accessible binding sites as a monolayer (Table S3), suggesting inaccessibility of most binding sites likely resulting from restriction of diffusion into the film. Additionally, the relationship between sensitivity and domain spacing mirrors that found in buffer, as 3xSP9.6k and 3xSP30.3k films greatly restrict SA diffusion and perform worse than the monolayer, while the 3xSP77.6k urine sample performance is indistinguishable from that of the monolayer. The one outlier to this trend is the 3xSP77.6k blood sample, which displays a nearly 2-fold reduction in LOD compared to the Sso monolayer (Figure 6f). This enhanced performance may be attributable to the larger size of proteins in blood than in urine,[23,24] enabling SA to diffuse into the thin films faster than a greater fraction of proteins in the blood.

In the tested biological fluids, the small protein mSA2 could be detected with LOD values 2 orders of magnitude lower than those obtained when using a simple monolayer as the biosensor (Figure 6c−f). Whereas the sensitivity of the monolayer in the fluids was up to an order of magnitude worse than in buffer, the thin films showed no change or slight improvement in sensitivity. Though the linear ranges for these sensors cannot be fully calculated from the data set, estimates of these ranges also suggest that the conjugate thin films have significantly wider linear ranges than the monolayer (Table S4). The apparent improvement in thin-film performance is likely a consequence of using slightly thicker films for the experiments performed in biological fluids (Table S3). Indeed, more binding sites were accessible in these samples than in those used for buffer experiments (Tables S2-3). $K_{d,app}$ values were also consistently lower in the thin films than in the monolayers, implying that less nonspecific binding occurred in the thin films due to the greater exclusion of proteins larger than mSA2 (Table S3). As expected, the $K_{d,app}$ values increased with increasing domain spacing, corresponding to more proteins being able to penetrate films with larger domain spacings. These findings further demonstrate that domain spacing can be tuned to allow selective uptake of small proteins.

The sensing capabilities of the designed protein−polymer conjugate thin-film biosensors provide substantial improvements to sensing in biological fluids compared to existing technologies. While previous studies have demonstrated that precisely designing the surface morphology of biosensors can allow sensitive analyte detection in the presence of other proteins,[11,12] these works either do not test their devices in mixtures of more than a few proteins[12] or show signal reduction when measurements are conducted in biological fluids.[11] In contrast, protein−polymer conjugate thin films exhibit no substantial reduction in signal or sensitivity when detecting a small protein in either serum or urine. As a more direct comparison to the biosensors developed in this study, porous silicon biosensors have been reported that act as both a filter and a substrate for biomolecule detection in whole blood.[48] Although the size of the silicon pores can be tuned to only permit molecules below a certain size to enter the pores (analogous to the domain spacing of polymer domains in protein−polymer conjugate thin films), nonspecific binding is still a potential issue. Blocking agents and wash buffers are required to prevent off-target molecules that are small enough to diffuse into the pores from blocking surface binding sites. Because protein−polymer conjugate thin films contain binding sites not only on the surface of the device but also throughout

DOI: 10.1021/acssensors.9b01020
ACS Sens. XXXX, XXX, XXX−XXX

the entire volume of the films, however, no blocking agents or rinsing steps are required to prevent nonspecific binding.

Sensor Stability. The developed biosensors displayed excellent stability for a protein-based sensor. When exposed to ambient conditions, films showed no significant decrease in binding capabilities over 4 weeks (Figure S8a). Furthermore, when stored at 60 °C and 60% relative humidity, the films were still able to bind analyte to 50% of their original capacity after 2 weeks, only becoming completely inactive after 4 weeks. The exceptional temperature stability is unsurprising, given that the Sso protein used as the molecular recognition element in these biosensors was engineered from a protein native to a hyperthermophilic microbe and was previously demonstrated to be resistant to extreme temperatures.[45] GISAXS linecuts indicated that no structural change had occurred in the films after 2 weeks (Figure S8b), suggesting that the decrease in binding capability was the result of 3xSso denaturing without causing microstructural rearrangement.

Sandwich Assay Demonstration. To demonstrate that the thin-film biosensors could be used in detection formats beyond simple imaging of fluorescently labeled analytes, model sandwich assays were performed in the films. Specifically, these tests were designed to demonstrate the feasibility of using the films for multistep detection assays such as a sandwich ELISA. The general procedure for this proof-of-concept experiment is illustrated in Figure 7. Films were first exposed to SA solutions and rinsed to remove unbound analyte. Taking advantage of the strong interaction between SA and biotin, thin films were then submerged in a solution of biotinylated horseradish peroxidase (biotin-HRP). Bound SA was detected colorimetrically through the HRP-mediated oxidation of 3,3′,5,5′-tetramethylbenzidine (TMB). Attempts to perform this assay using mSA2 as the analyte were unsuccessful, even when run on an Sso monolayer. Binding experiments with fluorescently labeled biotin-HRP revealed extremely weak binding between biotin and mSA2 (Figure S9), which is consistent with previous reports of the biotin−mSA2 dissociation constant being multiple orders of magnitude greater than that for biotin and streptavidin.[46,49]

When SA was applied to the bioconjugate films in the buffer, the films generally performed as well as a monolayer (Figure 8). In contrast to the findings using fluorescent assays, 3xSP9.6k films achieved essentially the same LOD as an Sso monolayer, while the LOD attained with 3xSP77.6k films was nearly twice as large. LOD was also found to be effectively independent of film thickness, giving a sensitivity that only varied based on the conjugate used to fabricate the film.

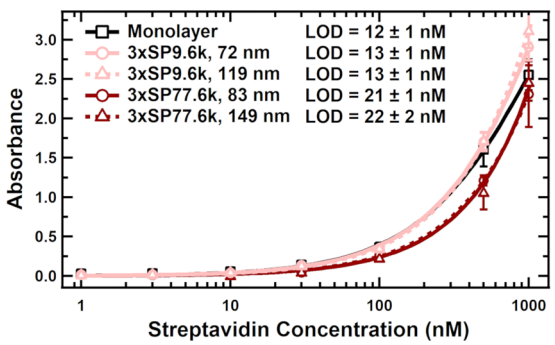

Figure 8. Binding curves for sandwich assays performed with SA in PBS. Error bars represent the standard deviation of three replicates.

Together, these results suggest that detection only occurred within a thin layer at the film surface. If diffusion limitations were significant enough to restrict analyte access to the majority of the film volume, the absorbance in 3xSP77.6k films would be predicted to consistently be less than that in 3xSP9.6k films due to the lower fraction of binding sites in the former films (Table 1). This expectation is consistent with experimental observations and is reasonable when considering that in these experiments, HRP was also required to diffuse into the films to observe a signal. The relatively large size of HRP (44 kDa) combined with likely steric hindrance from SA molecules bound to the film may have resulted in restrictions to diffusion greater than that in one-step fluorescent binding assays.

Sandwich assays exposed to SA in urine and blood serum gave similar results to those found using fluorescent assays. As was observed in the fluorescent assays (Figure 6a), LODs for all tested thin films were similar to that of a monolayer when SA was dissolved in 50% urine (Figure S10a). For SA samples in 50% blood serum, the LOD values for 3xSP9.6k and 3xSP30.3k films were 2-fold greater than that for an Sso monolayer (Figure S10b), again mirroring results for the fluorescent assays (Figure 6b). Unlike the fluorescent assays, however, for which 3xSP77.6k films were found to give a slight improvement in LOD, these same films resulted in a 2-fold greater LOD than a monolayer in the sandwich assays, possibly due to additional diffusion limitations for HRP. Though sandwich assay experiments could not be performed using mSA2 as the analyte, the general similarities between findings for fluorescent and sandwich assays suggest that sandwich assays with a smaller analyte would yield improved LOD values relative to a monolayer. Regardless, model sandwich assays using SA still demonstrate that these assays are feasible in the fabricated conjugate thin films.

CONCLUSIONS

3xSso-PNIPAM thin films display an apparent size-based diffusional resistance for proteins entering the film. Experiments performed with both mSA2 and the larger protein SA reveal that SA experiences greater resistance to diffusion into the films. In all cases, SA either demonstrates a longer timescale for diffusion into the thin films or requires films with larger domain spacings to allow appreciable uptake. By varying the molecular weight of the polymer block in the protein−polymer conjugates used to create the thin films, domain spacing can be adjusted to tune the size of proteins that the films could uptake. This simple tuning method should allow the facile design of biosensors optimized for the uptake of a target analyte.

The size-based uptake properties of the bioconjugate thin films are also found to enable greatly enhanced biosensor performance in biological fluids. Not only do these films achieve an LOD an order of magnitude lower than that of a traditional surface-immobilized protein biosensor in the buffer, but also the LOD is found to be up to 2 orders of magnitude lower for detection in biological fluids due to minimization of nonspecific binding events. Model sandwich assays performed in the thin films generally match results in fluorescent binding assays, demonstrating the potential for application in a variety of detection formats. With their easily tunable structure and highly sensitive detection capabilities, the designed protein−polymer conjugate thin films represent an extremely promising

DOI: 10.1021/acssensors.9b01020
ACS Sens. XXXX, XXX, XXX−XXX

technology for the detection of small proteins and peptides (molecular weight < ca. 15 kDa) in biological matrices.

■ ASSOCIATED CONTENT

Supporting Information

The Supporting Information is available free of charge on the ACS Publications website at DOI: 10.1021/acssensors.9b01020.

Polymer synthesis, protein expression and bioconjugation, sample characterization protocols, fluorescent labeling methodology, equations for GISAXS linecut and fluorescent binding assay curve-fitting, and additional analytical results (PDF)

■ AUTHOR INFORMATION

Corresponding Author

*E-mail: bdolsen@mit.edu. Tel.: 1-617-715-4548.

ORCID

Xue-Hui Dong: 0000-0002-6395-3103

Bradley D. Olsen: 0000-0002-7272-7140

Notes

The authors declare no competing financial interest.

■ ACKNOWLEDGMENTS

This work was supported by grants from the National Science Foundation (DMR-1253306) and the United States Defense Threat Reduction Agency (HDTRA1-16-1-0038). We thank Dr. Zhang Jiang for GISAXS experimental assistance at APS beamline 8-ID-E at Argonne National Laboratory. We also thank Dr. Masafumi Fukuto and Dr. Ruipeng Li for SAXS experimental assistance at NSLS-II beamline 11-BM at Brookhaven National Laboratory. We thank Dr. Hadley Sikes for use of an inverted fluorescence microscope. The Biophysical Instrumentation Facility for the Study of Complex Macromolecular Systems (NSF-0070319) is gratefully acknowledged for use of a CD spectrometer. Spectroscopic ellipsometry was conducted at the Institute for Soldier Nanotechnologies. The authors also thank Dr. Carla Thomas for assistance with PNIPAM synthesis.

■ REFERENCES

(1) Byrne, B.; Stack, E.; Gilmartin, N.; O'Kennedy, R. Antibody-Based Sensors: Principles, Problems and Potential for Detection of Pathogens and Associated Toxins. *Sensors* **2009**, *9*, 4407.

(2) Gebauer, M.; Skerra, A. Engineered protein scaffolds as next-generation antibody therapeutics. *Curr. Opin. Chem. Biol.* **2009**, *13*, 245−255.

(3) Binz, H. K.; Amstutz, P.; Plückthun, A. Engineering novel binding proteins from nonimmunoglobulin domains. *Nat. Biotechnol.* **2005**, *23*, 1257.

(4) Zhao, W.; Brook, M. A.; Li, Y. Design of Gold Nanoparticle-Based Colorimetric Biosensing Assays. *ChemBioChem* **2008**, *9*, 2363−2371.

(5) Grieshaber, D.; MacKenzie, R.; Vörös, J.; Reimhult, E. Electrochemical Biosensors - Sensor Principles and Architectures. *Sensors* **2008**, *8*, 1400.

(6) Fan, X.; White, I. M.; Shopova, S. I.; Zhu, H.; Suter, J. D.; Sun, Y. Sensitive optical biosensors for unlabeled targets: A review. *Anal. Chim. Acta* **2008**, *620*, 8−26.

(7) Hoa, X. D.; Kirk, A. G.; Tabrizian, M. Towards integrated and sensitive surface plasmon resonance biosensors: A review of recent progress. *Biosens. Bioelectron.* **2007**, *23*, 151−160.

(8) Nguyen, H. H.; Park, J.; Kang, S.; Kim, M. Surface Plasmon Resonance: A Versatile Technique for Biosensor Applications. *Sensors* **2015**, *15*, 10481−10510.

(9) Arlett, J. L.; Myers, E. B.; Roukes, M. L. Comparative advantages of mechanical biosensors. *Nat. Nanotechnol.* **2011**, *6*, 203−215.

(10) Masson, J.-F. Surface Plasmon Resonance Clinical Biosensors for Medical Diagnostics. *ACS Sensors* **2017**, *2*, 16−30.

(11) Jo, J.; Yoon, J.; Lee, T.; Cho, H.-Y.; Lee, J.-Y.; Choi, J.-W. H2O2 biosensor consisted of hemoglobin-DNA conjugate on nanoporous gold thin film electrode with electrochemical signal enhancement. *Nano Convergence* **2019**, *6*, 1.

(12) Lee, J.-H.; Park, B.-S.; Ghang, H.-G.; Song, H.; Yang, S. Y. Nano-Protrusive Gold Nanoparticle-Hybridized Polymer Thin Film as a Sensitive, Multipatternable, and Antifouling Biosensor Platform. *ACS Appl. Mater. Interfaces* **2018**, *10*, 13397−13405.

(13) Wisniewski, N.; Reichert, M. Methods for reducing biosensor membrane biofouling. *Colloids Surf. B. Biointerfaces* **2000**, *18*, 197−219.

(14) Haun, J. B.; Yoon, T.-J.; Lee, H.; Weissleder, R. Magnetic nanoparticle biosensors. *Wiley Interdiscip. Rev.: Nanomed. Nanobiotechnol.* **2010**, *2*, 291−304.

(15) Tekin, H. C.; Gijs, M. A. M. Ultrasensitive protein detection: a case for microfluidic magnetic bead-based assays. *Lab Chip* **2013**, *13*, 4711−4739.

(16) Desai, T. A.; Hansford, D. J.; Leoni, L.; Essenpreis, M.; Ferrari, M. Nanoporous anti-fouling silicon membranes for biosensor applications. *Biosens. Bioelectron.* **2000**, *15*, 453−462.

(17) Yuan, C.-J.; Hsu, C.-L.; Wang, S.-C.; Chang, K.-S. Eliminating the Interference of Ascorbic Acid and Uric Acid to the Amperometric Glucose Biosensor by Cation Exchangers Membrane and Size Exclusion Membrane. *Electroanalysis* **2005**, *17*, 2239−2245.

(18) Wang, S.; Sarenac, D.; Chen, M. H.; Huang, S.-H.; Giguel, F. F.; Kuritzkes, D. R.; Demirci, U. Simple filter microchip for rapid separation of plasma and viruses from whole blood. *Int. J. Nanomed.* **2012**, *7*, 5019−5028.

(19) Thorslund, S.; Klett, O.; Nikolajeff, F.; Markides, K.; Bergquist, J. A hybrid poly(dimethylsiloxane) microsystem for on-chip whole blood filtration optimized for steroid screening. *Biomed. Microdevices* **2006**, *8*, 73−79.

(20) Pfäfflin, A.; Schleicher, E. Inflammation markers in point-of-care testing (POCT). *Anal. Bioanal. Chem.* **2009**, *393*, 1473.

(21) Saito, Y.; Nakao, K.; Itoh, H.; Yamada, T.; Mukoyama, M.; Arai, H.; Hosoda, K.; Shirakami, G.; Suga, S.-i.; Minamino, N.; Kangawa, K.; Matsuo, H.; Imura, H. Brain natriuretic peptide is a novel cardiac hormone. *Biochem. Biophys. Res. Commun.* **1989**, *158*, 360−368.

(22) Murphy, M. P.; LeVine, H. Alzheimer's Disease and the β-Amyloid Peptide. *J. Alzheimer's Dis.* **2010**, *19*, 311.

(23) Schenk, S.; Schoenhals, G. J.; de Souza, G.; Mann, M. A high confidence, manually validated human blood plasma protein reference set. *BMC Med. Genomics* **2008**, *1*, 41.

(24) Adachi, J.; Kumar, C.; Zhang, Y.; Olsen, J. V.; Mann, M. The human urinary proteome contains more than 1500 proteins, including a large proportion of membrane proteins. *Genome Biol.* **2006**, *7*, R80.

(25) Burkert, S.; Bittrich, E.; Kuntzsch, M.; Müller, M.; Eichhorn, K.-J.; Bellmann, C.; Uhlmann, P.; Stamm, M. Protein Resistance of PNIPAAm Brushes: Application to Switchable Protein Adsorption. *Langmuir* **2010**, *26*, 1786−1795.

(26) Rodriguez-Emmenegger, C.; Brynda, E.; Riedel, T.; Houska, M.; Šubr, V.; Alles, A. B.; Hasan, E.; Gautrot, J. E.; Huck, W. T. S. Polymer Brushes Showing Non-Fouling in Blood Plasma Challenge the Currently Accepted Design of Protein Resistant Surfaces. *Macromol. Rapid Commun.* **2011**, *32*, 952−957.

(27) Chen, W.-L.; Cordero, R.; Tran, H.; Ober, C. K. 50th Anniversary Perspective: Polymer Brushes: Novel Surfaces for Future Materials. *Macromolecules* **2017**, *50*, 4089−4113.

(28) Blackman, L. D.; Varlas, S.; Arno, M. C.; Houston, Z. H.; Fletcher, N. L.; Thurecht, K. J.; Hasan, M.; Gibson, M. I.; O'Reilly, R. K. Confinement of Therapeutic Enzymes in Selectively Permeable

DOI: 10.1021/acssensors.9b01020
ACS Sens. XXXX, XXX, XXX−XXX

Polymer Vesicles by Polymerization-Induced Self-Assembly (PISA) Reduces Antibody Binding and Proteolytic Susceptibility. *ACS Cent. Sci.* **2018**, *4*, 718−723.
(29) Blackman, L. D.; Varlas, S.; Arno, M. C.; Fayter, A.; Gibson, M. I.; O'Reilly, R. K. Permeable Protein-Loaded Polymersome Cascade Nanoreactors by Polymerization-Induced Self-Assembly. *ACS Macro Lett.* **2017**, *6*, 1263−1267.
(30) Yoshikawa, C.; Goto, A.; Tsujii, Y.; Fukuda, T.; Kimura, T.; Yamamoto, K.; Kishida, A. Protein Repellency of Well-Defined, Concentrated Poly(2-hydroxyethyl methacrylate) Brushes by the Size-Exclusion Effect. *Macromolecules* **2006**, *39*, 2284−2290.
(31) Halperin, A. Polymer Brushes that Resist Adsorption of Model Proteins: Design Parameters. *Langmuir* **1999**, *15*, 2525−2533.
(32) Chrambach, A.; Rodbard, D. Polyacrylamide Gel Electrophoresis. *Science* **1971**, *172*, 440−451.
(33) Urueña, J. M.; Pitenis, A. A.; Nixon, R. M.; Schulze, K. D.; Angelini, T. E.; Gregory Sawyer, W. Mesh Size Control of Polymer Fluctuation Lubrication in Gemini Hydrogels. *Biotribology* **2015**, *1-2*, 24−29.
(34) Lieleg, O.; Ribbeck, K. Biological hydrogels as selective diffusion barriers. *Trends Cell Biol.* **2011**, *21*, 543−551.
(35) Paloni, J. M.; Miller, E. A.; Sikes, H. D.; Olsen, B. D. Improved Ordering in Low Molecular Weight Protein−Polymer Conjugates Through Oligomerization of the Protein Block. *Biomacromolecules* **2018**, *19*, 3814−3824.
(36) Thomas, C. S.; Olsen, B. D. Coil fraction-dependent phase behaviour of a model globular protein−polymer diblock copolymer. *Soft Matter* **2014**, *10*, 3093−3102.
(37) Lam, C. N.; Kim, M.; Thomas, C. S.; Chang, D.; Sanoja, G. E.; Okwara, C. U.; Olsen, B. D. The Nature of Protein Interactions Governing Globular Protein−Polymer Block Copolymer Self-Assembly. *Biomacromolecules* **2014**, *15*, 1248−1258.
(38) Thomas, C. S.; Glassman, M. J.; Olsen, B. D. Solid-State Nanostructured Materials from Self-Assembly of a Globular Protein−Polymer Diblock Copolymer. *ACS Nano* **2011**, *5*, 5697−5707.
(39) Thomas, C. S.; Xu, L.; Olsen, B. D. Kinetically Controlled Nanostructure Formation in Self-Assembled Globular Protein−Polymer Diblock Copolymers. *Biomacromolecules* **2012**, *13*, 2781−2792.
(40) Lam, C. N.; Olsen, B. D. Phase transitions in concentrated solution self-assembly of globular protein−polymer block copolymers. *Soft Matter* **2013**, *9*, 2393−2402.
(41) Dong, X. H.; Obermeyer, A. C.; Olsen, B. D. Three-Dimensional Ordered Antibody Arrays Through Self-Assembly of Antibody−Polymer Conjugates. *Angew. Chem., Int. Ed.* **2017**, *56*, 1273−1277.
(42) Chang, D.; Huang, A.; Olsen, B. D. Kinetic Effects on Self-Assembly and Function of Protein−Polymer Bioconjugates in Thin Films Prepared by Flow Coating. *Macromol. Rapid Commun.* **2017**, *38*, No. 1600449.
(43) Dixit, C. K.; Vashist, S. K.; MacCraith, B. D.; O'Kennedy, R. Multisubstrate-compatible ELISA procedures for rapid and high-sensitivity immunoassays. *Nat. Protoc.* **2011**, *6*, 439.
(44) Schneider, C. A.; Rasband, W. S.; Eliceiri, K. W. NIH Image to ImageJ: 25 years of image analysis. *Nat. Methods* **2012**, *9*, 671.
(45) Miller, E. A.; Traxlmayr, M. W.; Shen, J.; Sikes, H. D. Activity-based assessment of an engineered hyperthermophilic protein as a capture agent in paper-based diagnostic tests. *Mol. Syst. Des. Eng.* **2016**, *1*, 377−381.
(46) DeMonte, D.; Drake, E. J.; Lim, K. H.; Gulick, A. M.; Park, S. Structure-based engineering of streptavidin monomer with a reduced biotin dissociation rate. *Proteins: Struct., Funct., Bioinf.* **2013**, *81*, 1621−1633.
(47) Baumann, H.; Knapp, S.; Lundbäck, T.; Ladenstein, R.; Härd, T. Solution structure and DNA-binding properties of a thermostable protein from the archaeon Sulfolobus solfataricus. *Nat. Struct. Biol.* **1994**, *1*, 808.
(48) Bonanno, L. M.; DeLouise, L. A. Whole blood optical biosensor. *Biosens. Bioelectron.* **2007**, *23*, 444−448.
(49) Lim, K. H.; Huang, H.; Pralle, A.; Park, S. Stable, high-affinity streptavidin monomer for protein labeling and monovalent biotin detection. *Biotechnol. Bioeng.* **2013**, *110*, 57−67.

DOI: 10.1021/acssensors.9b01020
ACS Sens. XXXX, XXX, XXX−XXX